# Stable Operation Strategy for Near-Zero Discharge Evaporation and Crystallization System of Coal Chemical Wastewater Based on Model Predictive Control (MPC)

**Jing Wang[1], Jie Cao[2], Zhaohui Huo[2], Junqi Hui[3], Zhiquan Wang[4]**
[1]Xi'an Shiyou University, Xi'an 710000, Shaanxi, China
[2]Shaanxi MBA School, Xi'an 710000, Shaanxi, China
[3]Yan'an University, Xi'an 716000, Shaanxi, China
[4]Xi'an University of Science and Technology, Xi'an 710054, Shaanxi, China

Corresponding author: Jing Wang (e-mail: 15609236657@163.com)

**ABSTRACT** With the increasing integration of intelligent sensing, industrial communication networks, and Electromagnetic Waves, Antennas and Propagation technologies in smart process industries, stable control of complex multivariable systems has become essential for reliable information acquisition and distributed decision-making. This study proposes a stable operation strategy for a near-zero discharge evaporation and crystallization system for coal chemical wastewater based on model predictive control (MPC). A discrete state-space model incorporating influent chemical oxygen demand, salt concentration disturbances, liquid level–concentration coupling, and steam network constraints is established to characterize the dynamic behavior of the process. A rolling optimization controller integrating feedforward compensation and quadratic programming is developed to coordinate feed flow, steam regulation, and circulation control under multiple operational constraints. Simulation and industrial validation demonstrate that the proposed strategy reduces liquid level overshoot by 82.4%, decreases steam consumption fluctuation by 66.1%, and maintains stable operation with a water reuse rate above 92.3% under severe disturbance conditions. The results confirm that the MPC-based framework significantly enhances disturbance rejection, robustness, and energy efficiency while providing an effective engineering solution for cyber–physical industrial systems. Furthermore, the proposed architecture offers valuable references for communication-enabled intelligent monitoring, distributed sensing, and industrial automation applications associated with Electromagnetic Waves, Antennas and Propagation technologies.

**INDEX TERMS** model predictive control; industrial intelligent sensing; distributed monitoring; evaporation crystallization; coal chemical wastewater

## I. INTRODUCTION

UNDER the dual constraints of the national "dual-carbon" strategy and the ecological protection of the Yellow River Basin, the green and low-carbon transformation of the coal chemical industry has become an inevitable trend. The sector can achieve sustainable development while mitigating the environmental impact on the regional ecosystem [1-2]. Yanchang Petroleum Yulin Energy and Chemical Company, relying on the " integrated utilization of oil, gas, coal, and salt" model, has built the world's first integrated utilization project of coal, oil, and gas resources in the ecologically fragile area of northern Shaanxi, establishing the goal of "near-zero discharge" of wastewater and becoming a benchmark enterprise for water conservation. Through the development of water-saving technologies that maximize water conservation throughout the entire process, the annual raw water consumption is only 46% of the initial design, demonstrating significant results. However, with increasingly stringent environmental policies and increased production loads, the operation stability of the reclaimed water plant, as a key hub for the plant's water balance, is directly related to the safe and continuous production of the main unit. How to maintain the efficient and stable operation of the wastewater treatment system under complex operating conditions has become a core bottleneck restricting enterprises from further tapping into the potential for energy conservation and consumption reduction [3-4].

Since its commissioning in 2014, the near-zero discharge system for wastewater in the ecologically fragile area of northern Shaanxi has undergone hardware upgrades, including the addition of a quadruple-effect evaporator, buffer tank, and salt-drying pond, which have improved the treatment load. However, it still faces technical challenges such as drastic fluctuations in the influent quality of the main unit, large lag in the evaporation and crystallization process, and strong coupling. Traditional distributed PID control strategies are unable to cope with the dynamic interaction between multiple variables, especially when facing high-salt shock loads, which can easily lead to oscillations in the liquid level of the evaporation system or pressure imbalances in the steam pipeline network [5-6]. Operational practice shows that frequent fluctuations in the concentration and flow rate of the evaporation unit not only increase the operational difficulty of the subsequent solid-liquid separation unit and limit the release of the overall system treatment capacity, but also cause sudden changes in steam consumption due to control lag, which can interfere with the balance of the entire plant's steam pipeline network and pose a risk of the main unit being forced to reduce its load. In addition, the existing control logic lacks a global consideration of the operating limits of the equipment and the energy balance of the entire plant, making it difficult to meet the requirements of green factories for refined management and control [7-8].

MPC, as an advanced process control technology, has been widely used in the optimization of distillation towers and steam pipelines in the petrochemical industry, demonstrating significant advantages in handling systems with multiple constraints and large time delays [9-10]. However, in the field of coal chemical wastewater evaporation and crystallization, existing research on complex systems after hardware completion projects mainly focuses on single-equipment optimization, lacking a system-level control strategy that combines feedforward compensation for influent disturbances with utilization of steam waste heat. In particular, considering the dynamic characteristics changes of the Yulin Energy Chemical Company's reclaimed water plant after its transformation from a six-effect to a four-effect system, how to design an MPC algorithm that can explicitly handle steam pipeline pressure constraints, adapt to strong water quality disturbances, and is engineering-applicable remains to be explored in depth [11-12].

Therefore, this paper takes the evaporation and crystallization unit of the Yulin Energy Chemical Company's reclaimed water plant as the research object and proposes a stable operation strategy based on MPC. In this research, a state space model is first built to represent the variables affecting wastewater quality and process limitations, then an optimized rolling algorithm is developed to implement feedback control on flow rate based on influent concentration via real-time data; finally, the results are validated by running simulation studies and analyzing actual field data. It offers an engineering-based framework for achieving long-term stable wastewater management.

## II. PROCESS ANALYSIS AND MODELING OF NEAR-ZERO DISCHARGE SYSTEM FOR COAL CHEMICAL WASTEWATER

### *PROCESS FLOW OVERVIEW*

This study examine the nearly zero-liquid-discharge wastewater treatment system in the comprehensive utilization project of coal/oil/gas resources at the Yanchang Petroleum Yulin Energy and Chemical Company. This system began its official operation in September 2014 to help address the bottleneck of high concentration brine treatment for energy and chemical companies in ecologically fragile regions. The complete process flow structure consists of wastewater treatment, reclaimed water plant, multi-effect evaporation, crystallization, and miscellaneous salt disposal units. The reclaimed water plant has a critical role in the plant's water balance, where the reclaimed water treatment plant performs the primary function of further treating/water from the main production area. Table 1 shows some of the key parameters related to the Yanchang Petroleum Yulin Energy and Chemical Company Comprehensive Utilization of Coal/Oil/Gas Resources project.

To address issues such as unstable influent water quality and insufficient output of the six-effect evaporator, the company implemented upgrades to the reclaimed water plant. The system was retrofitted from a six-effect to a four-effect configuration to increase single-effect evaporation intensity and address severe pressure drop issues inherent in the original over-extended series structure, thereby improving the robustness of the system against fluctuating salt loads. The upgraded unit, including a buffer tank and salt-drying tank, became the core focus of the control strategy. The process flow mainly includes pretreatment, membrane concentration, multieffect evaporation (MEE), and crystallization drying. High-concentration brine, after pretreatment, enters the evaporation system, utilizing low-pressure steam from the plant's four pressure-level steam networks (S1, S2, S4, and S5) as a heat source. Water and salt separation is achieved through vacuum evaporation, with the condensate recycled for production and impurities disposed of via filter press.

### *SYSTEM DYNAMIC CHARACTERISTICS AND CONSTRAINT ANALYSIS*

The evaporation and crystallization process of coal chemical wastewater has typical characteristics of complex industrial processes, mainly manifested as large time delay, strong coupling and multiple constraints. These characteristics directly determine the choice of control strategy [13-14]. First, there is the large time delay. The evaporation and concentration process involves phase change, heat transfer and mass transfer. There is a significant time delay from steam flow rate regulation to liquid level or concentration response. Especially in the multi-effect evaporation series structure, the fluctuation of the previous effect is transmitted to the subsequent effect with a cumulative delay effect, and traditional PID control is difficult to suppress the disturbance

**TABLE 1.** Key parameters of the comprehensive utilization project of coal, oil and gas resources of Yanchang Petroleum Yulin Energy and Chemical Company

| Parameter Category | Specific Indicator | Value/Description |
|---|---|---|
| Feedstock & Product | Raw Material Composition | Coal, residual oil, and natural gas three-feed coupling |
| | Methanol Plant Capacity | 1.8 million tons/year |
| | Dimethyl Methanol to Olefins Plant Capacity | 600,000 tons/year methanol-to-olefins |
| | Direct Crystallization Plant Capacity | 1.5 million tons/year residual oil catalytic thermal cracking |
| | Polyolefin Capacity | 1.2 million tons/year |
| | Hydrogen-Carbon Complementary Gain | Increased methanol production by 300,000 tons/year |
| Energy & Water Consumption | Comprehensive Energy Consumption of Methanol | 1.20 tce3/t methanol |
| | Fresh Water Consumption per Ton of Methanol | 1.78 t/t methanol |
| | Maximum Annual Raw Water Consumption | 11.9 million m3 (design value 46%) |
| | Annual Water Savings | 7.596~11.196 million tons |
| Emission & Efficiency | CO2 Emissions per Ton of Methanol | 1.03 t/t methanol |
| | Energy Conversion Efficiency | 61.88% |
| | Carbon Resource Utilization Rate | 55.74% |
| | Annual CO2 Emission Reduction | 2.82 million tons |
| Utility Parameters | Steam Pipeline Pressure Rating | S1: 10.6MPa, S2: 4.0MPa, S4: 1.0MPa, S5: 0.5MPa |
| | Waste Heat Power Generation Capacity | 13MW+12MW |
| | Interconnection Points | 166 locations (73 above ground/93 underground) |
| Wastewater System | Near-Zero Emission Commissioning Time | September 2014 |
| | Evaporation System Retrofit Plan | Six-effect → Four-effect + buffer tank + salt drying tank |
| | Reclaimed Water Plant Design Load | Dynamically adjusted based on the peak discharge of the main unit |

in time. The time delay constant $\tau$ can be approximately expressed as the sum of thermal inertia and fluid transport time as shown in equation (1):

$$\tau = \sum_{i=1}^{n} \frac{C_{p,i} M_i}{U_i A_i} + t_{\text{transport}} \tag{1}$$

In the equation, $C_{p,i}$, $M_i$, $U_i$, and $A_i$ represent the specific heat capacity, mass, heat transfer coefficient, and heat transfer area of the i-th effect evaporator, respectively, and $t_{\text{transport}}$ represents the material transport delay.

Secondly, there is Strong Coupling, with dynamic interactions between multiple variables within the system. Changes in steam pressure not only affect the evaporation rate but also cause fluctuations in system vacuum, thus affecting the feed flow rate and concentrate concentration.

Furthermore, there are Multiple Constraints, with operation limited by equipment physical limits and the overall plant energy balance. On the one hand, the selection and configuration of large-scale key equipment determine the upper limits of evaporator temperature, compressor load, and other operating parameters; on the other hand, the steam consumption of the evaporation system must conform to the balance of the entire plant's steam network to avoid affecting the stable operation of the waste heat and pressure utilization power generation project. In particular, the pressures of the S4 and S5 steam networks must be maintained within a stable range to prevent impact on downstream users.

Finally, there are Strong Disturbances. The water quality of the main unit fluctuates drastically, especially the shock loads of chemical oxygen demand and salinity, which act directly on the system inlet as uncontrollable disturbances, placing extremely high demands on the robustness of the control system [15-16]. These characteristics together constitute the boundary conditions for MPC controller design.

## CONSTRUCTION OF MATHEMATICAL MODELS FOR CONTROL

To design the MPC strategy, a mathematical model reflecting the dynamic characteristics of the system needs to be established. Given the nonlinear characteristics of the evaporation crystallization system, this paper employs a linearization method near the equilibrium point to construct a discrete state-space model [17-18]. The system state variable vector $x(k) \in R^n$ is defined, including the liquid level $L_i$ of each evaporator effect, the concentrate concentration $C_i$, and the steam pressure $P_s$; the control input vector $u(k) \in R^m$ includes the feed flow rate $F_{\text{in}}$, the steam regulating valve opening $V_{\text{stm}}$, and the circulating pump frequency $f_{\text{pump}}$; the disturbance vector $d(k) \in R^p$ mainly consists of the influent concentration $C_{\text{in}}$ and the flow fluctuation $F_{\text{dist}}$; the system output vector $y(k) \in R^q$ represents the key monitoring indicators, liquid level and concentration.

Considering the dynamic response of the modified four-effect evaporation system, the discretized state-space equation is shown in equation (2):

$$\begin{cases} x(k+1) = Ax(k) + Bu(k) + Ed(k), \\ y(k) = Cx(k) + Du(k) \end{cases} \tag{2}$$

$A$ is the system state matrix, representing the dynamic characteristics of the process; $B$ is the control input matrix; $E$ is the disturbance matrix; $C$ is the output matrix; and $D$ is the direct transfer matrix. Matrix parameters are obtained from field step response test data.

For the MPC controller design, the prediction time domain $N_p$ and control time domain $N_c$ are defined. To simplify calculations, the multi-step prediction is expanded into matrix form, and the predicted output vector $Y(k)$ is shown in equation (3):

$$Y(k) = \Phi x(k) + \Gamma U(k) + \Lambda D(k) \tag{3}$$

In the equation, $Y(k)$ is the predicted output sequence, and $U(k)$ is the control sequence to be optimized. Matrices $\Phi$, $\Gamma$, and $\Lambda$ are formed by exponential operations of system matrices $A$, $B$, and $C$, representing the dynamic response trajectory of the system to future control actions and disturbances.

During model identification, special attention should be paid to the impact of influent concentration disturbances on the crystallization point of the concentrate. Through historical data regression analysis, a correlation model between concentration disturbances and evaporation rate is established, as shown in equation (4):

$$\Delta C_{\text{out}}(k) = \beta_1 \Delta C_{\text{in}}(k - \tau_d) + \beta_2 \Delta Q_{\text{steam}}(k) \quad (4)$$

$\tau_d$ is the disturbance delay time, and $\beta_1$ and $\beta_2$ are the identification coefficients. This model will serve as the basis for subsequent rolling optimization algorithms, enabling coordinated control of feed, steam, and pump frequency, and ensuring further exploration of the system's operational potential based on hardware modifications.

## III. MPC-BASED CONTROL STRATEGY DESIGN

### BASIC PRINCIPLES OF MODEL PREDICTIVE CONTROL

MPC, as a model-based advanced process control algorithm, has the core advantage of being able to explicitly handle constraints and large time delays in multivariable systems, which is highly compatible with the dynamic characteristics of coal chemical wastewater evaporation and crystallization systems [19-20]. In the control architecture constructed in this study, the MPC controller mainly includes three basic components: prediction model, rolling optimization, and feedback correction. The prediction model uses the established state-space equation to predict the system output trajectory in the future finite time domain based on the current system state $x(k)$ and control input sequence $u(k)$. In view of the significant time delay in the evaporation and crystallization process, MPC can predict the changing trends of liquid level and concentration in advance by setting an appropriate prediction time domain $N_p$, thereby overcoming the action delay of traditional feedback control [21-22]. The prediction trajectory considers the cumulative effect of control increment, as shown in equation (5):

$$y(k+i \mid k) = CA^i x(k) + \sum_{j=0}^{i-1} CA^{i-1-j} Bu(k+j \mid k) \quad (5)$$

In the equation, $i = 1, 2, \ldots, N_p$. This equation shows that the output at future moments depends not only on the current state but also on a series of future control actions. This foresight allows the controller to adjust the steam valve opening in advance before fluctuations in the main unit's incoming water quality reach the evaporation unit, achieving "preemptive control" [23-24].

The rolling optimization mechanism is the key difference between MPC and traditional control. At each sampling moment, the controller solves a finite-time open-loop optimization problem to obtain the optimal control sequence. However, only the first control variable u(k) in the sequence is executed, and the controller is re-optimized based on the new measurement value at the next moment. This "rolling" strategy allows the controller to adapt in real time to unpredictable disturbances such as fluctuations in the main unit's incoming water quality [25-26]. The model predictive control framework is shown in Figure 1:

In Figure 1, solid lines represent data flow and dashed lines represent constraints. The control structure takes the evaporation crystallization system as the controlled object and consists of a core control unit composed of modules such as a prediction model, rolling optimization, and feedback correction. The system establishes a prediction model based on the state-space model of the evaporation process to estimate the dynamic behavior of the system in the future prediction time domain. On this basis, the rolling optimization module uses the quadratic programming solution method to calculate the optimal control sequence that satisfies the performance index and constraints, and sends the control quantity at the current moment to the Distributed Control System (DCS) actuator to realize real-time adjustment of the steam valve and feed pump. At the same time, the system introduces a feedback correction link to correct the model prediction results based on the deviation between the actual output and the set value, so as to improve the control accuracy and robustness [27-28].

### FEEDFORWARD-INTEGRATED ROLLING OPTIMIZATION DESIGN

### PREDICTIVE MODEL AND FEEDBACK CORRECTION

The prediction model is based on discrete state-space equations, using the current state variable $x(k)$ and control sequence $u(k)$ to predict the liquid level and concentration trajectory in the future $N_p$ time domain. To address the significant hysteresis characteristic of the evaporation and crystallization process, the model overcomes the action delay of traditional feedback control through recursive calculation, ensuring the controller has foresight. To eliminate model mismatch and the influence of unmodeled dynamics, a feedback correction loop is introduced.

The feedback correction loop uses the deviation between the actual output $y(k)$ and the model prediction value to correct the model online, eliminating the influence of model mismatch and unmodeled dynamics. Considering the nonlinear characteristics of the evaporation unit in the reclaimed water plant, this paper adopts a linearized model combined with deviation compensation to ensure good prediction accuracy even under large fluctuations in operating conditions. Through this closed-loop correction mechanism, the system can effectively suppress the dynamic characteristic changes that may occur after the conversion from a six-effect evaporator to a four-effect evaporator, ensuring the robustness of the control strategy. The corrected prediction value $y_{\text{corr}}$ is calculated as shown in equation (6):

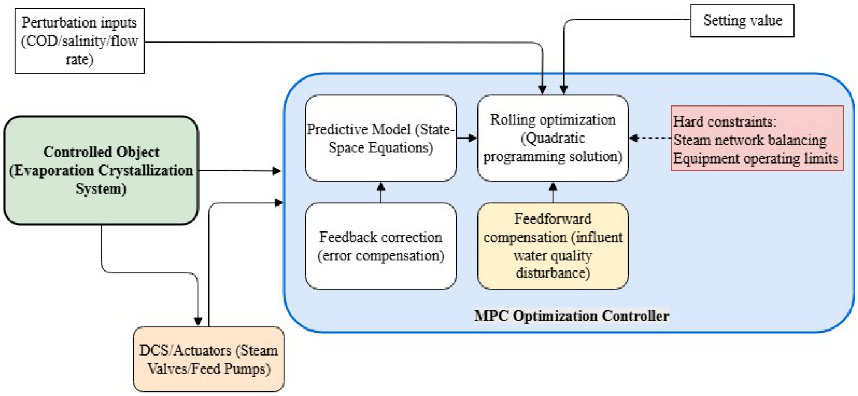


**FIGURE 1.** Model Predictive Control Framework: solid lines represent data flow and dashed lines represent constraints. The control structure takes the evaporation crystallization system as the controlled object and consists of a core control unit composed of modules such as a prediction model, rolling optimization, and feedback correction

$$y_{\text{corr}}(k+i \mid k) = y(k+i \mid k) + h_i \cdot e(k) \tag{6}$$

$e(k)$ represents the prediction error at the current moment, and $h_i$ is the correction coefficient.

### DESIGN OF MULTI-OBJECTIVE OPTIMIZATION FUNCTION

The controller's objective function is in the form of quadratic equation, in order to achieve a multiple objective collaborative optimization. It takes into account three fundamental measures which are based upon: output tracking error, penalty for control increment and economic energy consumption. The penalty for deviation from evaporator liquid level, concentrate concentration and water quality by ensuring that the water quality of the "near-zero discharge" system is within acceptable limits by using the $Q$ weight matrix as a penalty. Additionally, $R$ and $S$ weight matrices are applied as penalties to the quantity and absolute value of the quantity respectively. The amount of steam used is weighted heavily to ensure that the steam required for the plant to balance its steam network and use waste heat appropriately [29-30]. The specific form of the objective function is shown in equation (7):

$$\begin{aligned} J = & \sum_{i=1}^{N_p} \|y(k+i \mid k) - r(k+i)\|_Q^2 \\ & + \sum_{j=0}^{N_c-1} \|\Delta u(k+j \mid k)\|_R^2 \\ & + \lambda \sum_{j=0}^{N_c-1} \|u_{\text{steam}}(k+j \mid k)\|^2 \end{aligned} \tag{7}$$

In the equation, $r(k+i)$ is the setpoint trajectory; $\lambda$ is the energy consumption penalty coefficient.

To achieve the green plant construction goals of Yulin Energy Chemical Company, a steam consumption penalty term is specifically introduced, with a higher weight to respond to the plant's steam network balance requirements. Furthermore, a feedforward compensation mechanism is integrated, incorporating the online monitored influent COD and salinity signals as measurable disturbances into the optimization process. Addressing the core pain point of unstable influent water quality in the main unit, this paper designs a feedforward compensation stage, incorporating the online monitored influent COD and salinity signals as measurable disturbances into the prediction model to adjust the feed flow rate and steam valve opening in advance, thereby suppressing the impact of disturbances on the system output. The feedforward control law design is shown in equation (8):

$$u_{\text{ff}}(k) = -K_{\text{ff}} \cdot d(k) \tag{8}$$

$K_{\text{ff}}$ is the feedforward gain matrix, obtained by offline calculation of the inverse steady-state gain matrix of the output under disturbance. Feedforward control can adjust the feed flow rate and steam opening before the disturbance affects the output, significantly suppressing the interference of high-salt shock loads on system stability and achieving global optimization of energy consumption and stability.

### HARD CONSTRAINT HANDLING AND QUADRATIC PROGRAMMING SOLUTION

The constraints are directly derived from the actual limitations of the selection and configuration of large-scale key equipment. Hard constraints include the physical limits of the actuators, such as the steam regulating valve opening of 0% to 100% and the circulating pump frequency of 30 to 50 Hz; soft constraints involve process safety boundaries, such as the upper limit of the evaporator liquid level to prevent material leakage and the upper limit of the temperature to prevent equipment corrosion. In particular, considering the coupling relationship between the S4 and S5 steam pipelines in the plant area, the control strategy incorporates steam pressure fluctuations into the constraints to avoid the large-scale steam consumption of the evaporation system affecting the stable operation of the steam waste heat and pressure utilization power generation project. The mathematical description of the constraints is shown in equation (9):

$$\begin{cases} u_{\min} \le u(k+j \mid k) \le u_{\max}, \\ \mid \Delta u(k+j \mid k) \mid \ \le \Delta u_{\max}, \\ y_{\min} \le y_{\text{corr}}(k+i \mid k) \le y_{\max} \end{cases} \tag{9}$$

The optimization problem is transformed into a constrained quadratic programming (QP) problem, which is solved quickly using the effective set method [31-32]. Through this multi-variable coordinated control, MPC can tap the potential of the system after hardware modification while ensuring the safe operation of the equipment, solve the problem of insufficient output of the filter press system caused by neglecting one aspect in traditional control, and achieve global optimization of energy consumption and stability [33-34].

## IV. EXPERIMENTAL ANALYSIS

### SIMULATION PLATFORM SETUP AND SCENE SETTING

To verify the effectiveness of the proposed MPC strategy in the evaporation and crystallization system of coal chemical wastewater, this paper constructs a simulation environment and sets the model boundary conditions based on engineering parameters. The simulation model uses the constructed discrete state-space equations as its core, integrating an influent concentration disturbance module, a four-effect evaporation coupled dynamic module, and a steam pipeline pressure constraint module. Sampling will be done every 60 seconds to match the data refresh rate of the on-site DCS system. Model parameters are developed using data gathered from on-site step response tests, and are verified against historical operational data (2020-2023), providing confidence for the degree of consistency between the simulated conditions and actual production conditions, thus providing a reliable yardstick for evaluating the effectiveness of the control strategy.

The simulation scenario design is aimed at replicating the real life operating conditions of Yulin Energy Chemical Company's reclaimed water treatment facility, specifically those associated with the central theme of "unstable influent water quality in the main unit." In order to accomplish this, 3 typical types of disturbances were established: (1) step disturbance of COD of the influent (+/- 30% of design); (2) random fluctuations in influent flow rate (15% standard deviation); (3) combined fluctuation due to both fluctuation in water quality & flow at same time. The reference being used to compare against is the current distributed PID control employed within the industry, and the performance criteria evaluated against consist of three metrics: dynamic performance, steady state tracking accuracy , and energy efficiency.

### COMPARISON OF CONTROL PERFORMANCE UNDER NOMINAL OPERATING CONDITIONS

Table 2 shows a comparison of the dynamic performance indices of different control strategies under step disturbances:

Table 2 quantifies the performance advantages of the MPC strategy over traditional PID control from the perspective of time-domain response. Data shows that under a step disturbance in influent COD, MPC, through its feedforward compensation mechanism, shortens the rise time to 92.7 s and suppresses overshoot to within 4.2%, significantly better than PID control's 23.8%. This is mainly attributed to MPC's rolling optimization mechanism's ability to predict the dynamic coupling of liquid level and concentration in advance, avoiding the "lag-overshoot" cycle of traditional feedback control. Of particular note is the steam consumption fluctuation index; the MPC strategy reduces the fluctuation amplitude by 66.1%. This improvement is primarily due to the integrated feedforward compensation mechanism, which preemptively adjusts the steam regulating valve to cancel out influent quality disturbances before they propagate through the multi-effect system, rather than relying solely on reactive valve adjustments typical of PID control. This directly responds to the steam network balance constraints and ensures the stable operation of the plant's S4/S5 steam network.

Table 3 shows the comparison of key parameter fluctuation ranges under different disturbance intensities under the MPC strategy:

Table 3 evaluates the adaptability of the MPC strategy under different influent loads from the perspective of disturbance robustness. With an increase of the disturbance level between ±10% to ±30%, liquid level fluctuations increase from a range of 0.12~0.18 m to 0.38~0.62 m; however, all values are still below the evaporator's maximum allowable liquid level (0~1.5 m). Although the concentration deviation rises with increasing disturbance, the concentration of the concentrated stream remains below the crystallization point due to the constraint optimization feature of model predictive control (MPC), thus eliminating the ability for scaling or clogging to occur. In addition, the water reuse rate has remained above 92.3% under combined disturbance conditions, verifying the effectiveness of this water-savings oriented approach.

### DYNAMIC RESPONSE ANALYSIS UNDER WATER QUALITY DISTURBANCE

This paper looks into the operation means of how the MPC strategy increases stability for a evaporation crystallization. To do this, the study examines two aspects of the overall analysis: time domain response and frequency domain characteristics. The time domain analysis will look at how three critical states (liquid level, concentration, and vapor pressure) behave when they are disturbed together, and the frequency domain analysis will look at the stability margin of the closed-loop system and the level of disturbance that can be tolerated by the closed-loop system without causing a significant change. The time-domain response comparison results are shown in Figure 2.

Figure 2 displays the time domain responses of liquid level, concentration and steam pressure from two different

**TABLE 2.** Dynamic Performance of Different Control Strategies under Step Disturbances

| Performance Index | Evaluation Dimension | PID Control | Proposed MPC | Improvement |
|---|---|---|---|---|
| Rise Time (s) | Response speed | 186.3 | 92.7 | 50.2% |
| Overshoot (%) | Stability | 23.8 | 4.2 | 82.4% |
| Settling Time (s) | Convergence efficiency | 412.5 | 158.3 | 61.6% |
| Steady-State Error (%) | Tracking accuracy | 5.7 | 1.3 | 77.2% |
| Integral Absolute Error (m·s) | Overall performance | 1847.2 | 423.6 | 77.1% |
| Steam Consumption Fluctuation (%) | Energy consumption stability | 18.9 | 6.4 | 66.1% |

**TABLE 3.** Fluctuation Range of Key Parameters under Different Disturbance Intensities

| Disturbance Level | Liquid level fluctuation (m) | Concentration deviation (g/L) | Steam consumption fluctuation (t/h) | Water reuse rate (%) |
|---|---|---|---|---|
| Low strength (±10%) | 0.12~0.18 | 0.8~1.3 | 1.2~2.1 | 96.8~97.5 |
| Medium strength (±20%) | 0.21~0.35 | 1.5~2.8 | 2.3~4.6 | 95.2~96.7 |
| High strength (±30%) | 0.38~0.62 | 2.9~5.1 | 4.8~8.3 | 93.1~95.0 |
| Combined disturbance | 0.45~0.78 | 3.2~6.4 | 5.6~10.2 | 92.3~94.8 |

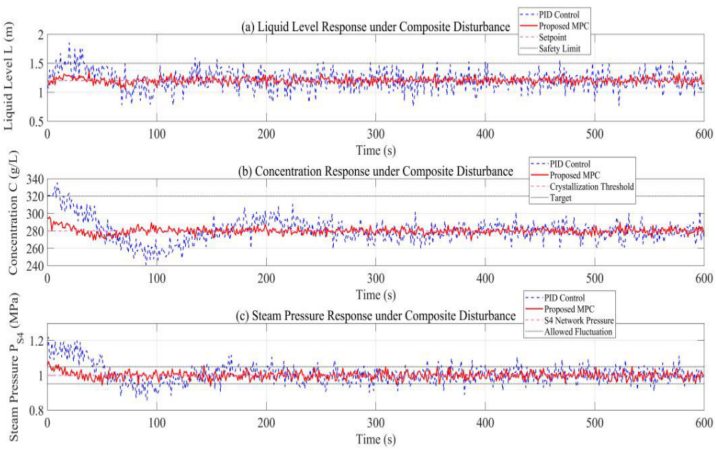


**FIGURE 2.** Time-domain Response Comparison: (a) liquid level; (b) concentration; (c) steam pressure

disturbances at the same time. Figure 2(a) shows the time domain response for liquid level, under PID control there is an oscillating liquid level range from 0.8 to 1.8 m, whereas the MPC controlled liquid level has been regulated to a much smaller range of approximately 1.2 m, thus giving smaller amplitude of oscillation also much shorter settling time than those observed with PID control. Figure 2(b) shows that MPC, through a feedforward compensation mechanism, keeps the concentration deviation consistently around the crystallization threshold, significantly reducing steady-state error and effectively avoiding the risk of evaporator scaling. Figure 2(c) further verifies the supporting role of MPC in balancing the steam pipeline network; the S4 steam pressure fluctuation meets the constraint requirement of avoiding impact on the steam waste heat and pressure utilization power generation project. The effect of the three-variable synergistic optimization indicates that the MPC strategy can systematically solve the limitations of traditional single-loop control's "one-sided" approach. The core reason is that the rolling optimization mechanism can predict the liquid level-concentration coupling dynamics in advance, and combined with feedforward compensation, achieves preemptive control of influent disturbances.

To further reveal the influence mechanism of control strategy on system stability margin and anti-interference capability at the frequency domain level, the frequency domain stability characteristics of PID and MPC closed-loop systems were compared based on the identified linearized model, and the results are shown in Figure 3.

As shown in Figure 3a, the amplitude-frequency response curves reveal that both control methods maintain high gain levels in the low-frequency region, indicating good tracking capability of the system to setpoint changes. However, as the frequency increases, the amplitude curve under MPC control decreases more smoothly, suggesting better filtering of high-frequency disturbances and thus improving operational stability. The phase-frequency response shown in Figure 3b illustrates that the MPC closed-loop system has a smoother phase change trend across all frequencies and has a substantially greater phase margin than that of the PID control strategy. This indicates that the system has a good stability margin when subjected to variations in the parameters or external disturbances. In contrast, the PID control's phase curve shows more phase lag at mid to high

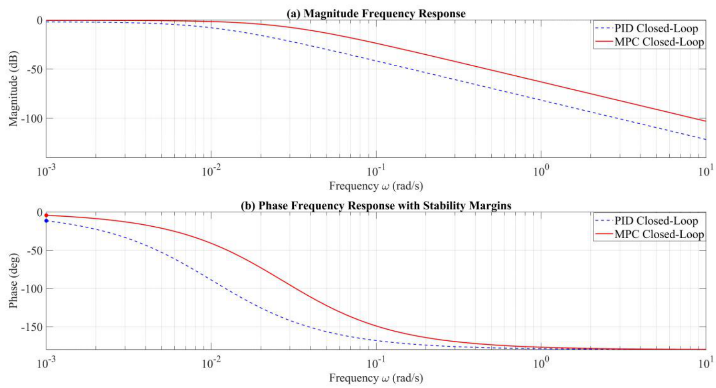


**FIGURE 3.** Frequency domain stability characteristics of PID and MPC closed-loop systems: (a) amplitude-frequency; (b) phase-frequency

frequencies and thus has a smaller relative stability margin. The analysis of both the amplitude-frequency and phase-frequency characteristics of the data leads to the conclusion that the implementation of the model predictive controller not only improves the disturbance suppression capability but also provides a larger stability margin, thereby providing a level of assurance that the multivariable coupled system will operate safely and stably during the evaporation process.

### *ROBUSTNESS VERIFICATION UNDER MODEL MISMATCH*

In actual industrial processes, uncertainties are introduced by factors such as model parameter identification errors, sensor measurement noise, and actuator aging. Figure 4 quantifies the impact of parameter uncertainty on control performance using Monte Carlo simulation.

Figure 4 shows the statistical distribution characteristics of the integral absolute error (IAE) of the two control strategies under parameter uncertainty. As can be seen from the probability density function (PDF) distribution in sub-Figure 4a, the IAE distribution range of the PID control is significantly wider, mainly concentrated between approximately 1500 and 2200, indicating that the system error fluctuates significantly under parameter disturbances. In contrast, the IAE distribution of the proposed MPC control strategy is significantly concentrated in the lower value region, with most samples located in the 300–600 range, showing a significant reduction in error and dispersion, indicating better control performance stability. Further observation from the cumulative distribution function in Figure 4b reveals that the difference between the two methods is more pronounced in the high quantile range, with the 90th percentile of the PID control being significantly lower than that of the MPC control.

The Nyquist response characteristic plots of the open-loop PID and MPC have been produced to further assess how perturbations in model parameters and unmodeled dynamics affect the stability of the closed-loop system. The Nyquist plots have been shown in Figure 5. Through comparison between their trajectory distribution in the complex plane and the relative locations of the uncertainty circle and critical point located at (-1,0), it is possible to quantitatively verify the robust stability margin of the proposed MPC strategy under uncertainties including, but not limited to, parameter identification errors from a frequency domain analysis.

The two control approaches are shown in Figure 5 as part of the open loop system's Nyquist response characteristics when there are model uncertainties present. The Nyquist trajectory for the PID controller predominantly lies within the left half of the complex plane; however, at low frequency, it approaches the critical point (-1, 0) which indicates the PID controller has a limited stability margin. The Nyquist curve for the MPC controller is mostly compressed to the origin and is very far from the critical point, indicating that the MPC structure has more than enough stability margin at the open loop level. At each of three frequencies, the plotted uncertainty circles represent the amount of disturbance that model multiplication uncertainties can create in the frequency response. Combining the Nyquist trajectory position and uncertainty distribution, it can be judged that, in the presence of parameter perturbations and modeling errors, the proposed MPC control strategy exhibits a higher safety margin in terms of robust stability, providing a more reliable guarantee for the stable operation of the system under complex operating conditions.

### *MULTI-OBJECTIVE OPTIMIZATION ASSESSMENT OF ENERGY AND WATER CONSUMPTION*

For near-zero discharge systems that treat wastewater produced from coal chemistry, optimizing energy use, water consumption and water quality is the primary goal. The three-dimensional response surface in figure 6 provides a visual means of the relationship between steam consumption and the rate of reducing/reusing water, as well as the effect of inflow load factors and disturbances; each shown with respective contour lines using the MPD microbial process control technique.

The response surface for steam consumption (figure 6a) shows that the amount of steam consumed generally in-

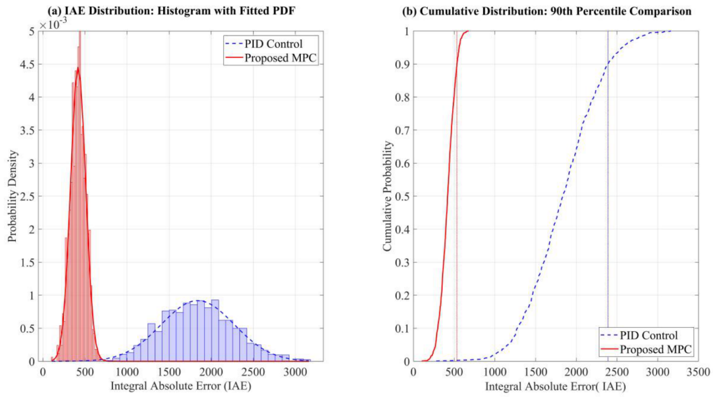


FIGURE 4. Impact of Parameter Uncertainty on Control Performance: (a) PDF of IAE; (b) CDF of IAE

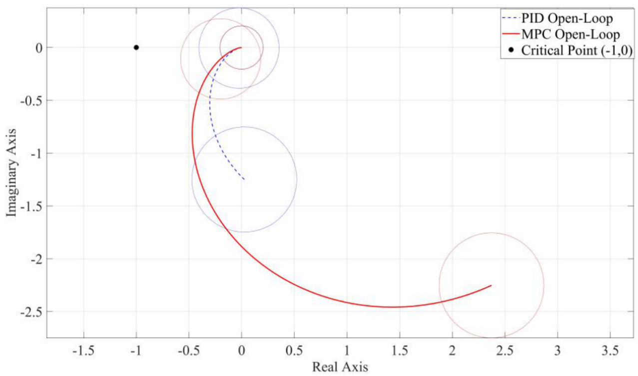


FIGURE 5. Robust Stability of the MPC Strategy

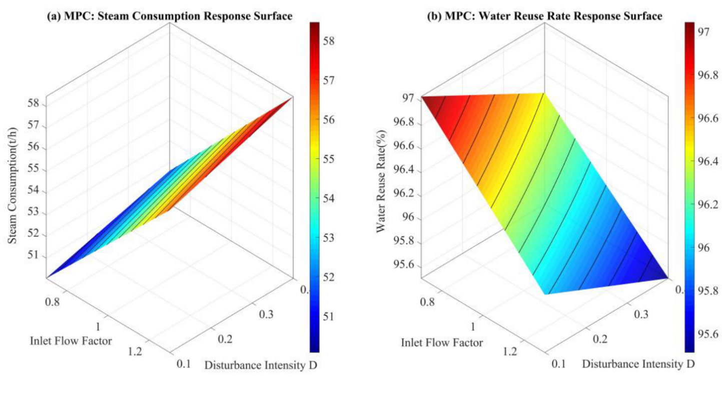


FIGURE 6. Response Surface of Steam Consumption and Water Reuse Rate: (a) steam consumption; (b) water reuse rate

creases as the feed flow rate factor increases. The magnitude of this increase is somewhat larger in the area of higher disturbance (D). Thus, at high load and strong disturbance, the system requires greater heat compensation to maintain stable operation. The smoothness of the steam consumption surface indicates that MPC is capable of achieving relatively stable energy regulation across multiple operating conditions. The response surface for water reuse rate (Figure 6b) demonstrates an inverse relationship to both feed load and disturbance intensity, with small decreases in water reuse rate as both factors increase. Nevertheless, the water reuse rate remains high overall, indicating that under complex operating conditions, the system still has a high degree of resource utilization. Both response surfaces display continuous and regular variation patterns throughout their respective parameter spaces, indicating that the developed model is representative of the system's operating characteristics. Comprehensive analysis shows that within a reasonable feed load and disturbance range, the MPC strategy can not only effectively control the increase in steam consumption

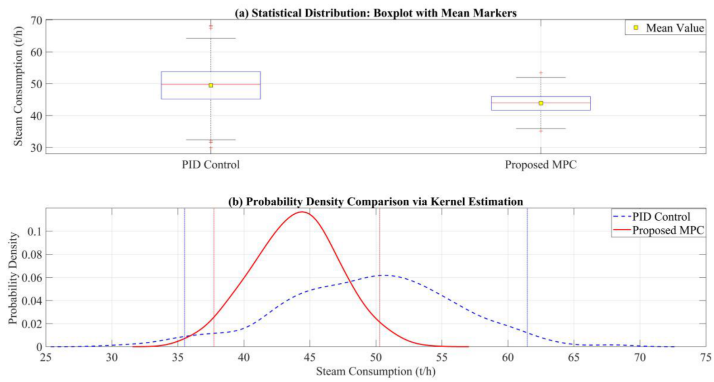


**FIGURE 7.** The Effect of the MPC Strategy on Suppressing the Volatility of Energy Consumption Indicators: (a) box plot; (b) kernel density

but also maintain high water reuse efficiency, providing an important basis for energy-saving optimization of the evaporation process.

Figure 7 uses a combination of box plots and kernel density estimation to statistically evaluate the effect of the MPC strategy on suppressing the volatility of energy consumption indicators.

As marked by figure 7a, there are a great deal of variances in PID control sample rates (median of ~49th t h, mean of ~50th t h, interquartile range of about the ~45′s to 53′s). There are also several outliers present indicating that there is a significant amount of fluctuation in energy usage when using this control method. When looking at the MPC control, the box height of energy consumption is much smaller (median of about ~44th t h, mean of ~44 to 45th t h, approximately 42 to 46th t h interquartile range) indicating that it has significantly less dispersion than PID control method does. This suggests that the MPC control tends to reduce the fluctuation range with multiple Monte Carlo simulations therefore providing a more stable method with more energy-saving abilities. Figure 7b provides insight into the energy consumption distribution probabilities of both control strategies. The diagrams were created using kernel density estimation techniques. The peak in the probability density diagram for the PID control lies primarily around the 49th -51st range while the distribution curve exhibits a relatively flat and long-tailed shape and has a 95% confidence interval of approximately 39-62 t h indicating that operating states of the system would be random. On the other hand, the probability density function for the MPC control system shows a peak concentration of probability density between 43 and 45 t/h, with a more peaked or sharper curve indicating that there is less variability in the measurements of steam consumption with MPC than with PID control. The 95 percent confidence interval for this distribution is approximately 37 to 51 t/h, indicating an even greater reduction in average levels of steam usage as well as a marked improvement in consistency and predictability of system operation due to the use of the MPC controller. These data further support the use of the proposed MPC controller as an effective means of improving energy efficiency through statistical analysis.

## V. CONCLUSION

This article describes how wastewater systems in the coal chemical are challenged by unpredictable input characteristics and the long precedences in evaporation and crystallization inherent to closed-loop designs. The purpose of the present paper is to develop a multivariate model predictive control (MPC) strategy to coordinate feed rate, steam consumption, and circulation pump frequency based on a closed-loop control system with process disturbances caused by influent concentration and steam network pressure. A rolling optimization scheme using feedforward compensation will be developed to provide a way to optimize each of these variables. The results show that the MPC strategy minimizes fluctuations in liquid level as well as optimizes steam consumption during a salt shock load event compared to conventional PID controls, thereby reducing the effects of control issues resulting from lag in downstream filtration. Additionally, the findings demonstrate that further improvements in system performance can be obtained through equipment modifications, establishing a viable method for coal chemical industries to achieve water conservation and emissions reduction goals, while transitioning to sustainable, smart plants. Furthermore, this control architecture possesses high scalability and can be deeply integrated with carbon data management platforms and finishing projects, achieving global optimization of the plant's water balance and ensuring enterprises maintain their status as national-level green factories and water-saving benchmarks.

## AUTHOR CONTRIBUTIONS

Conceptualization –Jing Wang, Jie Cao, Zhaohui Huo, Junqi Hui and Zhiquan Wang; methodology – Jing Wang, Jie Cao, Zhaohui Huo, Junqi Hui and Zhiquan Wang; investigation – Jing Wang, Jie Cao, Zhaohui Huo, Junqi Hui and Zhiquan Wang; writing-original draft preparation – Jing Wang, Jie Cao, Zhaohui Huo, Junqi Hui and Zhiquan Wang. All authors have read and agreed to the published version of the manuscript.

## CONFLICTS OF INTEREST

The authors declare no conflict of interest.

## FUNDING

This research received no external funding.

## ACKNOWLEDGEMENTS

Not applicable.

## REFERENCES

[1] Y. Zhang, H. Li, T. Ramirez Reina, et al., "Coal chemistry industry: from production of liquid fuels to fine chemicals to carbon materials," Energy & fuels, vol. 37, no. 23, pp. 17754-17764, 2023, doi: 10.1021/acs.energyfuels.3c02661.

[2] Y. Guo, L. Peng, J. Tian, et al., "Deploying green hydrogen to decarbonize Chinas coal chemical sector," Nature communications, vol. 14, no. 1, pp. 8104-8115, 2023, doi: 10.1038/s41467-023-43540-4.

[3] X. Liu, "Low-carbon utilization of coal gangue under the carbon neutralization strategy: a short review," Journal of Material Cycles and Waste Management, vol. 25, no. 4, pp. 1978-1987, 2023, doi: 10.1007/s10163-023-01712-w.

[4] T. Zhang, M. Zhang, L. Jin, et al., "Advancing carbon capture in hard-to-abate industries: technology, cost, and policy insights," Clean Technologies and Environmental Policy, vol. 26, no. 7, pp. 2077-2094, 2024, doi: 10.1007/s10098-024-02810-5.

[5] M. Tang, S. Zhang, Z. Bai, et al., "Power control of generator sets in coal-fired power plants based on the combination of MPC and neural network PID," Journal of Industrial and Management Optimization, vol. 22, no. 1, pp. 450-485, 2026, doi: 10.3934/jimo.2026017.

[6] P. Mohindru, "Review on PID, fuzzy and hybrid fuzzy PID controllers for controlling non-linear dynamic behaviour of chemical plants," Artificial Intelligence Review, vol. 57, no. 4, pp. 97-125, 2024, doi: 10.1007/s10462-024-10743-0.

[7] J. Huo, Z. Wang, C. Oberschelp, et al., "Net-zero transition of the global chemical industry with CO 2-feedstock by 2050: feasible yet challenging," Green Chemistry, vol. 25, no. 1, pp. 415-430, 2023, doi: 10.1039/D2GC03047K.

[8] M. Jiang, Y. Cao, C. Liu, et al., "Tracing fossil-based plastics, chemicals and fertilizers production in China," Nature Communications, vol. 15, no. 1, pp. 3854-3866, 2024, doi: 10.1038/s41467-024-47930-0.

[9] A. Znad O, O. Mohamed, and A. Elhaija W, "Speeding-up startup process of a clean coal supercritical power generation station via classical model predictive control," Process Integration and Optimization for Sustainability, vol. 6, no. 3, pp. 751-764, 2022, doi: 10.1007/s41660-022-00243-5.

[10] Q. Li, L. Yu, T. Liu, et al., "Enhancing Efficiency in Coal-Fired Boilers Using a New Predictive Control Method for Key Parameters," Sensors, vol. 26, no. 1, pp. 330-348, 2026, doi: 10.3390/s26010330.

[11] D. He, W. Zhan, Y. Kang, et al., "Gaussian process-based economic MPC with delay compensation for sncr-scr combined denitration systems," Industrial & Engineering Chemistry Research, vol. 63, no. 45, pp. 19628-19639, 2024, doi: 10.1021/acs.iecr.4c02065.

[12] U. Shah, A. Paulson J, and R. Bakshi B, "Real-time synergies between homeostatic technological and homeorhetic ecological systems by multiscale MPC and Bayesian optimization," Industrial & Engineering Chemistry Research, vol. 63, no. 49, pp. 21389-21403, 2024, doi: 10.1021/acs.iecr.4c02417.

[13] Y. Yu, J. Hou, A. Jahanger, et al., "Decomposition analysis of Chinas chemical sector energy-related CO2 emissions: From an extended SDA approach perspective," Energy & Environment, vol. 35, no. 5, pp. 2586-2607, 2024, doi: 10.1177/0958305X231151682.

[14] A. Bashir M, T. Ji, J. Weidman, et al., "Plastic waste gasification for low-carbon hydrogen production: a comprehensive review," Energy Advances, vol. 4, no. 3, pp. 330-363, 2025, doi: 10.1039/D4YA00292J.

[15] X. Wu, Y. Dong, J. Zhao, et al., "Distribution, sources, and ecological risk assessment of polycyclic aromatic hydrocarbons in surface water in the coal mining area of northern Shaanxi, China," Environmental Science and Pollution Research, vol. 30, no. 17, pp. 50496-50508, 2023, doi: 10.1007/s11356-023-25932-7.

[16] H. An, Z. Liu, and S. Mu, "Process analysis of a novel coal-to-methanol technology for gasification integrated solid oxide electrolysis cell (SOEC)," International Journal of Hydrogen Energy, vol. 48, no. 26, pp. 9805-9811, 2023, doi: 10.1016/j.ijhydene.2022.11.300.

[17] L. Ting T, W. Hasanah N, S. Rohman F, et al., "Modeling and control of steam methane reforming process using model predictive control," ASEAN Journal of Process Control, vol. 2, no. 1, pp. 1-13, 2023.

[18] M. Tang, B. An, J. Qiu, et al., "Multi-model predictive control of SCR flue gas denitrification system in coal-fired power plant based on kernel fuzzy c-means clustering and integrated model," The Canadian Journal of Chemical Engineering, vol. 102, no. 2, pp. 748-764, 2024, doi: 10.1002/cjce.25082.

[19] J. Wang, B. Ding, and P. Wang, "Modeling and finite-horizon mpc for a boiler-turbine system using minimal realization state-space model," Energies, vol. 15, no. 21, pp. 7935-7955, 2022, doi: 10.3390/en15217935.

[20] Y. Jia, Y. Dong Z, C. Sun, et al., "A tube-based distributed MPC based method for low-carbon energy networks with exogenous disturbances," IEEE Transactions on Network Science and Engineering, vol. 12, no. 1, pp. 381-391, 2024, doi: 10.1109/TNSE.2024.3497577.

[21] H. Hou, M. Gan, X. Wu, et al., "Real-time energy management of low-carbon ship microgrid based on data-driven stochastic model predictive control," CSEE Journal of Power and Energy Systems, vol. 9, no. 4, pp. 1482-1492, 2023.

[22] B. Decardi-Nelson and J. Liu, "Robust economic MPC of the absorption column in post-combustion carbon capture through zone tracking," Energies, vol. 15, no. 3, pp. 1140-1159, 2022, doi: 10.3390/en15031140.

[23] Z. Hou, L. Chu, W. Du, et al., "A novel dual-model MPC-based energy management strategy for fuel cell electric vehicle," IEEE Transactions on Transportation Electrification, vol. 10, no. 4, pp. 8585-8604, 2024, doi: 10.1109/TTE.2024.3369081.

[24] M. Shen, B. Tang, and K. Zhang, "Low carbon operation optimisation strategies for heating, ventilation and air conditioning systems in office buildings," International Journal of Production Research, vol. 62, no. 18, pp. 6781-6800, 2024, doi: 10.1080/00207543.2024.2325582.

[25] H. Ni, Y. Wang, X. Tang, et al., "An Intelligent Two-Stage Dispatch Framework for Cost and Carbon Reduction in Multi-Energy Virtual Power Plants," Processes, vol. 14, no. 5, pp. 743-763, 2026, doi: 10.3390/pr14050743.

[26] I. Beloglazov and V. Plaschinsky, "Development MPC for the grinding process in SAG mills using DEM investigations on liner wear," Materials, vol. 17, no. 4, pp. 795-820, 2024, doi: 10.3390/ma17040795.

[27] Z. Yang, F. Yang, W. Hu, et al., "Delay compensation control strategy for electric vehicle participating in frequency regulation based on MPC algorithm," Electronics, vol. 11, no. 15, pp. 2341-2357, 2022, doi: 10.3390/electronics11152341.

[28] H. Fan, E. Lu, W. Yu, et al., "Multi-agent deep reinforced co-dispatch of energy and hydrogen storage in low-carbon building clusters," IEEE Transactions on Network Science and Engineering, vol. 11, no. 6, pp. 5449-5462, 2023, doi: 10.1109/TNSE.2023.3243202.

[29] N. Degiuli, I. Martić, and G. Grlj C, "Slow Steaming as a Sustainable Measure for Low-Carbon Maritime Transport," Sustainability, vol. 16, no. 24, pp. 11169-11186, 2024, doi: 10.3390/su162411169.

[30] R. Cownden, D. Mullen, and M. Lucquiaud, "Towards net-zero compatible hydrogen from steam reformation-Technoeconomic analysis of process design options," International Journal of Hydrogen Energy, vol. 48, no. 39, pp. 14591-14607, 2023, doi: 10.1016/j.ijhydene.2022.12.349.

[31] R. Quirynen, S. Safaoui, and S. Di Cairano, "Real-time mixed-integer quadratic programming for vehicle decision-making and motion planning," IEEE Transactions on Control Systems Technology, vol. 33, no. 1, pp. 77-91, 2024, doi: 10.1109/TCST.2024.3449703.

[32] X. Cao, X. Pu, C. Hua, et al., "Neural dynamics for constrained bi-objective quadratic programming with applications to scientific computing," Tsinghua Science and Technology, vol. 30, no. 5, pp. 2014-2028, 2025, doi: 10.26599/TST.2024.9010152.

[33] H. Lu and J. Yang, "A practical and optimal first-order method for large-scale convex quadratic programming: H," lu, j. yang. Mathematical Programming, vol. 215, no. 1, pp. 771-808, 2026, doi: 10.1007/s10107-025-02241-0.

[34] Y. Fang, S. Na, W. Mahoney M, et al., "Fully stochastic trust-region sequential quadratic programming for equality-constrained optimization problems," SIAM Journal on Optimization, vol. 34, no. 2, pp. 2007-2037, 2024, doi: 10.1137/22M1537862.